Air Quality, Atmosphere & Health (2022) 15:1547–1556
https://doi.org/10.1007/s11869-022-01201-3

PM10, PM2.5, PM1, and PM0.1 resuspension due to human walking

Ahmed Benabed[1] · **Amir Boulbair**[2,3]

Received: 25 January 2022 / Accepted: 9 April 2022 / Published online: 18 April 2022

Abstract

Indoor air quality has become a major concern in recent years due to the adverse effects of poor air quality, caused by the presence of several sources of pollutants, on the building occupants' health. Particle resuspension has been identified as a major indoor particle matter (PM) source in indoor environments. The present work investigated the human walking-induced PM resuspension in a full-scale laboratory experimental chamber. The PM mass concentration was monitored using a Mini-wras Grimm counter. The floor of the test chamber was covered with a tufted synthetic carpet and uniformly loaded with neutralized alumina dust. Using the mass-based balance equation and the well-mixed condition hypothesis, resuspension rates were estimated after 10 min of walking activity. Results show that human walking significantly increases the indoor PM10, PM2.5, PM1, and PM0.1 concentrations. The average estimated PM10, PM2.5, PM1, and PM0.1 resuspension rates were $(2.5 \pm 0.6) \times 10^{-1}$ h^{-1}, $(1.9 \pm 0.5) \times 10^{-2}$ h^{-1}, $(6.5 \pm 0.3) \times 10^{-3}$ h^{-1}, and $(4.3 \pm 0.3) \times 10^{-3}$ h^{-1}, respectively.

Keywords Indoor air quality · Well-mixed condition · PM (particle matter) · Loss rate · Particle resuspension · Resuspension rate

Nomenclature

V	Volume of the test chamber (m^3)
C_{in}	PM concentration in the test chamber (µg/m^3)
C_{out}	PM outdoor concentration (µg/m^3)
r_{rs}	PM resuspension rate (h^{-1})
A_{rs}	Shoe sol area (m^2)
L	PM concentration on the floor (floor loading) (µg/m^2)
a_r	Air change rate (h^{-1})
β	PM deposition coefficient (h^{-1})
λ_{loss}	PM loss rate (h^{-1})
f_{rs}	Walking rate (steps/h)

Introduction

Humans are becoming more aware of the indoor air quality (IAQ) importance. This awareness is driven by the fact that they spend most of their time indoors, where they may be exposed to potentially harmful pollutants for a long time. Some of these indoor pollutants have a negative impact on our comfort, cognitive performance, and health in general (Mendell 2007). Many studies directly link the size of particles to their potential for causing health problems (Peters et al. 1997). Air pollution is responsible for many pathologies such as allergies, asthma, pulmonary infections, and cardiovascular diseases (Araujo et al. 2008; Diaz-Sanchez et al. 2003; Ferin 1994; Verrier et al. 2002). Using data on the mortality of more than 500,000 people, Pope et al. (2002) concluded that an increase in exposure to air pollutants of 10 µg m^{-3} in fine particles led to increases of 4%, 6%, and 8% in the risks of developing a pathology, having heart problems, and developing lung cancer, respectively. In addition, British researchers have recently shown the link between ultrafine particles found in the human brain and Alzheimer's disease (Maher et al. 2016). Even more, in the context of the current health crisis, researchers have shown that exposure to air pollution is a comorbid factor of SARS-COV-2 (Coccia 2020; Conticini et al. 2020; Ogen 2020; Wu et al. 2020).

✉ Ahmed Benabed
ahmed.benabed@estaca.fr

[1] Department of Mechanical and Environmental Engineering, ESTACA, Paris-Saclay Campus, 78180 Montigny-le-Bretonneux, France

[2] LAMIH, UMR 8201, Univ. Polytechnique Hauts-de-France, CNRS, F-59313 Valenciennes, France

[3] Av M. Crépeau, LaSIE, University of La Rochelle, 17042 La Rochelle, Cedex 01, France

Indoor air is a mixture of a multitude of solid particles, or liquid droplets called particulate matter (PM). According to their aerodynamic diameter, particles are classified as fine particles, including PM10 (particles with an aerodynamic diameter smaller than 10 µm), PM2.5 (particles with an aerodynamic diameter smaller than 2.5 µm), and PM1 (particles with an aerodynamic diameter smaller than 1 µm), or ultrafine particles, including PM0.1 (particles with an aerodynamic diameter smaller than 10 µm). PM levels in indoor environments can be influenced by numerous factors such as indoor sources, ventilation, outdoor conditions, particle deposition, and particle re-suspension from surfaces (Thatcher 1995). It has been found that human activity such as walking can increase concentration of particles in indoor environments (Luoma and Batterman 2001; Qian et al. 2014).

During the last 10 years, several experimental and numerical works have been carried to understand and quantify this phenomenon. Luoma and Batterman (2001) found that human walking was the main reason for the concentration change of 24–55% particulate matter with a particle size of 1–25 µm in a non-smoking room. Braniš et al. (2005) reported that human activities in a classroom contribute significantly to increase the particle concentration especially PM2.5 and PM10. Serfozo et al. (2014) measured the mass and number concentration of PM10 during walking experiments inside a laboratory. The calculated average resuspension rate was found ranging from 10^{-2} to10^{-3} h^{-1}. The estimated resuspension rate was found independent of the initially deposited surface dust loading.

Despite the considerable efforts to understand and quantify PM resuspension phenomenon, there are still several uncertainties particularly about the resuspension of particle smaller than 0.1 µm. This is in part due to the complex nature of particles, in terms of their sources, mechanisms of formation, and their chemical compositions. Another part of this complexity stems from the complexity of PM resuspension process itself (Benabed et al. 2020a). Furthermore, PM0.1 range has not been systematically considered by the scientific community in this field. It has even been confirmed that this range is not related to an indoor human activity such as human walking. This shortage is in our opinion due to two main reasons: first, the measurements were generally carried out in uncontrolled environments with high background noise and/or in the presence of other indoor sources which may hide the contribution of human walking. Second, the measuring instruments used during the experiments are mainly optical counters. These latter are generally limited to particle sizes larger than 0.1 µm. Therefore, additional works are always necessary. The goal of this work is to study human walking-induced particle resuspension in a full-scale chamber. Indoor and outdoor mass concentrations of four fractions, PM10, PM2.5, PM1, and PM0.1, were monitored using particle counters. The walking activity for each experiment was carried out by an adult participant for a period of 10 min. The floor was covered with a tufted synthetic carpet and previously loaded with a neutralized standard ISO 12103–1 A2 dust. The particle resuspension rate coefficients were estimated using the mass balance equation and the hypothesis of a well-mixed indoor condition.

Methods and materials

Experiment design and instrumentation

The experiments were carried out in a full-scale wooden chamber (see Fig. 1). The test chamber (chamber 1 in Fig. 1) has a floor area of 2.5 m × 2.5 m and an internal volume of 15.62 m^3. The floor was covered with a tufted synthetic carpet (see Fig. 2). The latter is class 22 which means that it

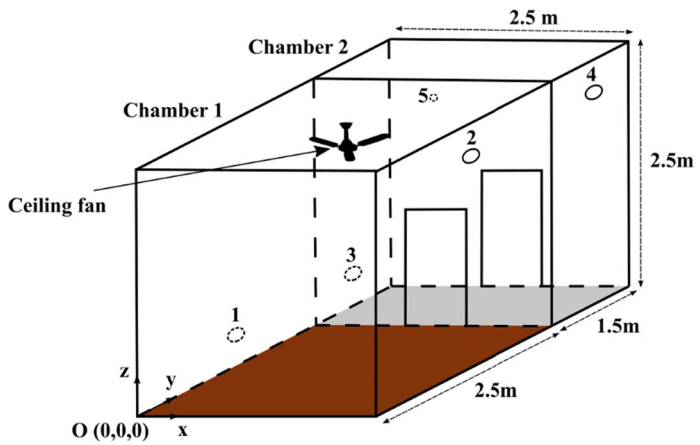

Fig. 1 Sketch of the experimental chamber

1: Air supply (chamber 1) (x, y, z) = (0, 1.25, 0.35) m 2: Air return (chamber 1) (x, y, z) = (2.5, 1.25, 2.15) m
3: Air supply (chamber 2) (x, y, z) = (0, 3.25, 0.35) m 4: Air return (chamber 2) (x, y, z) = (2.5, 3.25, 2.15) m
5: Aerosol injection (x, y, z) = (1.25, 2.5, 2.25) m

Fig. 2 Image of the carpet simple

Table 1 Characteristics of the carpet

Total thickness (mm)	Fiber high (mm)	Backing	Density (points/m^2)	Composition	Antistatic
8	6	Two back surfaces	43,750	Polypropylene	Yes

is suited for domestic usage (living room, hallway, corridor, or even the bathroom). Table 1 presents some characteristics of the carpet used as flooring in this work. The test chamber was ventilated by an inlet and an outlet of air situated on two opposite walls. A second wooden chamber (chamber 2 in Fig. 1) with dimensions of $2.5 \times 1.5 \times 2.5$ m was placed in front of the test chamber to prevent contamination of this later. Low PM concentration levels in chamber 2 were maintained. The low levels of PM concentration were maintained in chamber 2 by injecting filtered air (using a 0.01 µm air filer) before and during the walking experiment.

ISO 12103–1 A2 Alumina powder was selected to seed the flooring to represent the range of resuspended particles relevant to human health. These polydisperse particles have the molecular formula Al_2O_3 and a density of 3950 kg/m^3. Figure 3a–b represent the size distribution and the fractions with respect to the total mass. In one hand, the $\frac{dN}{dlogD}$ size distribution of the alumina powder (see Fig. 3a) indicates that most of the particles belonged to the smaller particle classes (0.01–0.5 µm). On the other hand, $\frac{dM}{dlogD}$ distribution indicates that 0.3–10 µm particles dominate the total particle mass. Figure 3b indicates that over 92% of the total alumina powder consisted of PM10. Furthermore, PM0.1 represented a minor fraction of the total mass (about 0.39%).

Particle injecting was insured by a dispersion unit of TOPAS SAG 410 aerosol disperser. This later consists of a dual-stream ejector nozzle (similar to DIN ISO 5011) and a connecting tube for compressed air supply. Forces created in this ejector disperse the powder as a form of aerosol. In order to condition the charge distribution of the injected aerosol, an electrostatic aerosol neutralizer, SAG EAN 581, was connected in series of the ejector nozzle. The SAG EAN 581 is mainly based on the corona discharge principle and includes a mixing chamber with two separate ionizing heads and a control unit. Positive and negative ions are produced by the two ion blowers and mixed with the aerosol flow in the mixing compartment. A particle-free compressed air source is connected to the two ionizing heads and the mains voltage is connected to the power supply cord. The aerosol was injected on the top of the test chamber by a Bev-line antistatic tube and immediately mixed in the test chamber

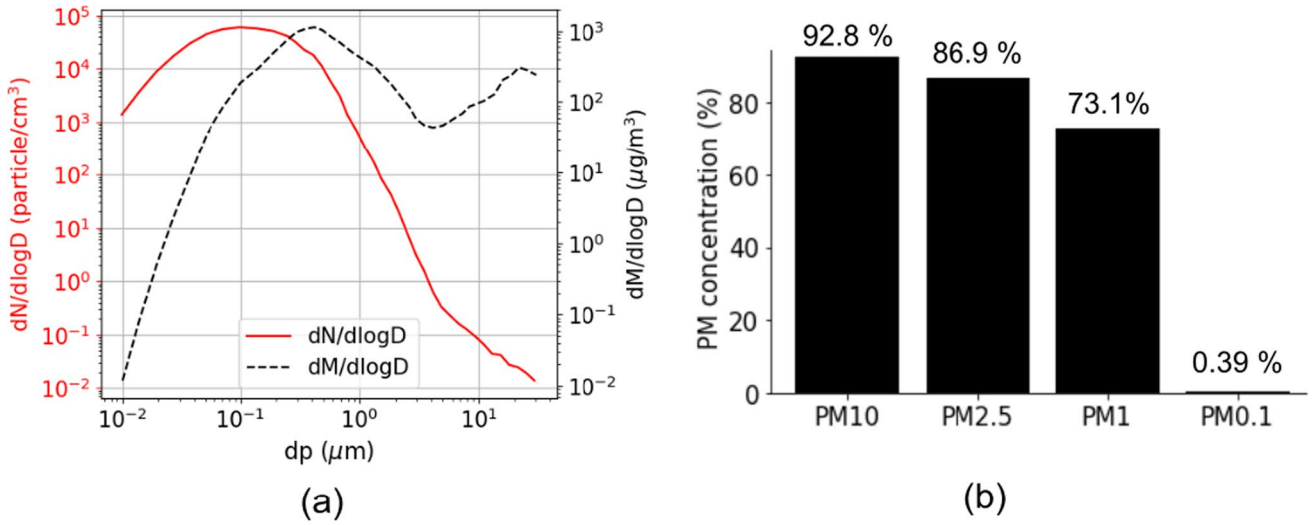

Fig. 3 Distribution of the alumina power **a** $\frac{dN}{dlogD}$,$\frac{dM}{dlogD}$, **b** fractions as a function of the total mass

by a three-blade propeller ceiling fan. This latter rotates at a speed of 450 rpm.

Particle concentration measurement in the two chambers was carried out using two Grimm monitors model Miniwras (see Fig. 4a). The latter combine two different types of measurement instruments: an aerosol spectrometer for particles larger than 0.253 µm and the so-called Nano-sizer for particles smaller than 0.253 µm. This monitor provides particle concentrations of 41 sizes ranging from 0.01 to 38.16 µm (see Table 2), enabling the investigation of a large range of particle sizes. The mass concentrations of all particle sizes were estimated using the particle number concentrations provided by the monitor and the density of alumina (particles are supposed to be spherical). Thus, the mass concentrations of PM10, PM2.5, PM1, and PM0.1 were found by summing the concentration of all particles smaller than 0.1 µm, 1 µm, 2.5 µm, and 10 µm respectively. Relative humidity and temperature were maintained at $35-40 \pm 0.1\%$ and 23 ± 0.1 °C during all experiments respectively. Measurement of these two parameters was carried out using a KIMO KCC 320 sensor (see Fig. 4b).

Particle deposition and resuspension study

In general, the resuspension rate cannot be directly estimated; however, it can be obtained by integrating the mass balance equations (rate change of particle concentration in the chamber and on the surface floor). In this work, the variation of the PM mass concentration inside the test chamber and on the carpet was modeled using the two-compartment balance model (Eq. (1)) (Benabed et al. 2020b; Lai et al. 2017; Qian and Ferro 2008). Certain assumptions are required to use this model:

1. The concentration is homogenous within the test chamber (well-mixed condition);
2. The distribution of particles on the carpet surface is uniform;
3. The concentration of particles outside the test chamber is insignificant;
4. The particle agglomeration is negligible;
5. No indoor sources;
6. Participant contribution is negligible;
7. The particle size distribution remains unchanged between the injection into the chamber and the deposition on the surface.

$$\begin{cases} V\frac{dC_{in,i}(t)}{dt} = -\left(a_r + \beta_i\right)VC_{in,i}(t) + RS_i(t) \\ A\frac{dL_i(t)}{dt} = -RS_i(t) + \beta_i VC_{in,i}(t) \end{cases} \quad (1)$$

where

V, volume of the test chamber (m^3);

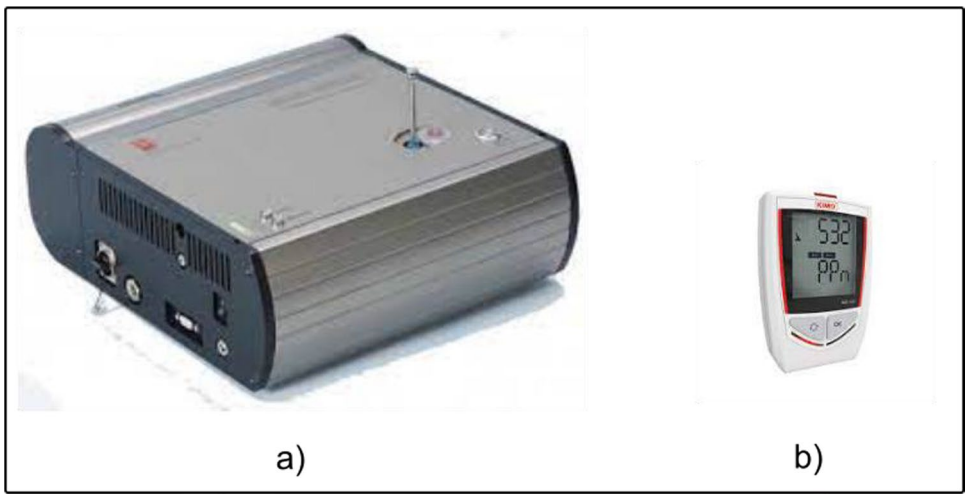

Fig. 4 **a** The Miniwras monitor, **b** KIMO KCC 320 sensor

Table 2 Particle sizes given by the Miniwras monitor (nm)

10	14	19	27	37	52	72
100	139	193	274.58	323	381	449.48
530.18	625.38	737.02	867.18	1000.0	1205.86	1424.96
1679.58	1978.13	2332.27	2745.80	3238.77	3817.43	4499.40
5307.20	6253.83	7370.21	8685.62	10,240.20	12,069.47	14,226.56
16,773.33	19,768.32	23,301.0	27,467.18	32,375.50	38,162.42	

$C_{in,i}$, PM concentration in the test chamber (i designates 10, 2.5, 1, or 0.1) (μg/m^3);

a_r, air change rate (h^{-1});

β_i :, PM deposition coefficient (h^{-1});

L_i, particle concentration on the floor (floor loading) (μg/m^2).

The term $RS_i(t) = r_{rs,i} f_{rs} A_{rs} L_i(t)$ in Eq. (1) represents the mass emission rate for PM resuspension at time t (μg/h). This term is considered a source for Eq. (1) and as a sink for Eq. (1). where $r_{rs,i}$ is the particle resuspension rate (h^{-1}), A_{rs} the shoe sol area (m^2), and f_{rs} the walking rate (steps/h).

The resuspension rate was derived from Eq. (1) as shown in Eq. (2):

$$\mathrm{r_{rs,i}(t)} = \frac{\mathrm{V}}{\mathrm{f_{rs} A_{rs} L_i(t)}} \left(\frac{\mathrm{dC_{in,i}(t)}}{\mathrm{dt}} + \lambda_{\mathrm{loss,i}} \mathrm{C_{in,i}(t)} \right) \tag{2}$$

where $\lambda_{loss} = a_r + \beta_i$ represents the loss rate (h^{-1}).

By rearranging the floor loading equation in Eq. (1), we can write:

$$\mathrm{A_{rs}} \frac{\mathrm{dL_i(t)}}{\mathrm{dt}} = -\mathrm{V} \left(\frac{\mathrm{dC_{in,i}(t)}}{\mathrm{dt}} + \mathrm{a_r C_{in,i}(t)} \right) \tag{3}$$

The surface loading at time t can be evaluated by integrating Eq. (3) from time 0 to t as shown in Eq. (4):

$$\mathrm{L_i(t)} = \mathrm{L_i(0)} - \frac{\mathrm{V}}{\mathrm{A_{rs}}} \left(\mathrm{C_{in,i}(t)} - \mathrm{C_{in,i}(0)} + \mathrm{a_r} \int_0^{\mathrm{t}} \mathrm{C_{in,i}(t')dt'} \right) \tag{4}$$

where $L_i(0)$ is the initial floor loading (μg/m^2).

Finally, the resuspension rate and the floor loading at time t were calculated resolving simultaneously Eq. (5)

$$\begin{cases} r_{rs,i}(t+\Delta t) = \frac{V}{f_s A_s L_i(t)} \left(\frac{C_{in,i}(t+\Delta t) - C_{in,i}(t)}{\Delta t} + \lambda_{loss,i} C_{in,i}(t) \right) \\ L_i(t) = L_i(0) - \frac{V}{f_s A_s} \left(C_{in,i}(t) - C_{in,i}(0) + a_r \int_0^t C_{in,i}(t') dt' \right) \end{cases} \tag{5}$$

Loss rate coefficient estimation

The loss rate coefficients were evaluated as follows: the total surfaces of the chamber, ceiling, and walls were carefully cleaned, the chamber was sealed, the fan was switched on, and the 0.05 g of alumina was injected in the test chamber. PM concentrations were monitored for a period of 90 min (from the time the powder was injected). The loss rate was then estimated by exponentially regressing the measured PM concentration (Benabed et al. 2020b). Experiment was repeated 5 times for each case to evaluate the repeatability of the measurements.

Air change rate

The air change rate was previously determined using carbon dioxide as a tracer gas and a KIMO KCC 320 sensor by following these steps: first, CO_2 was injected inside the experimental chamber; then, the KCC sensor was turned on and the chamber was sealed. The air change rate is then estimated by an exponential regression of the CO_2 concentration in the chamber.

Particle resuspension study

In this work, the resuspension rates were estimated following two steps:

Step 1: First, all internal surfaces were cleaned using a vacuum cleaner. During this time, the ventilation system was turned-on at full speed to evacuate particles that were resuspended during the cleaning process and to prevent them from being redeposited on the floor after the cleaning. This step was repeated 3 times to ensure a thorough cleaning of the surfaces. Second, the chamber was sealed, the ceiling fan was turned on, and a mass of 12.5 ± 10^{-5} g of alumina powder was injected (as an aerosol) inside the chamber. After 17 h, purified air was injected in test chamber for 6 h to reduce the background concentration.

Step 2: Once the two particle monitors were turned on, a participant entered the chamber 2, put on a previously cleaned suit and shoes (see Fig. 5a), and then waited for 10 min. The participant then accessed the test chamber and waited 5 min to confirm that any concentration changes within the chamber did not result from the door opening. The participant walked for 10 min at a rate of 48 steps/min following the path shown in Fig. 5b, and then sat for 5 min. After sitting for 5 min, the particle counter was turned off. For each studied case, the resuspension experiment was repeated 5 times to evaluate the repeatability of the measurements.

Floor loading estimation

The floor loading estimation after the injection of 12.5 ± 10^{-5} g of alumina powder (as described previous section) was conducted separately of the resuspension study. Deposited particles were collected using a miniature vacuum cleaner. The latter was repeatedly passed over the surface section to ensure that all deposited particles were collected. In order to verify the uniformity of the deposition of the dust on the floor, sampling was performed at four separate areas of the floor selected randomly. All the selected surfaces have an area of 0.25 m^2. The sampled powder and the filter were then weighed using a balance with a precision of 10^{-5} g. The collected powder mass was then deduced by subtracting the initial filter mass m_0. This step was then repeated 3

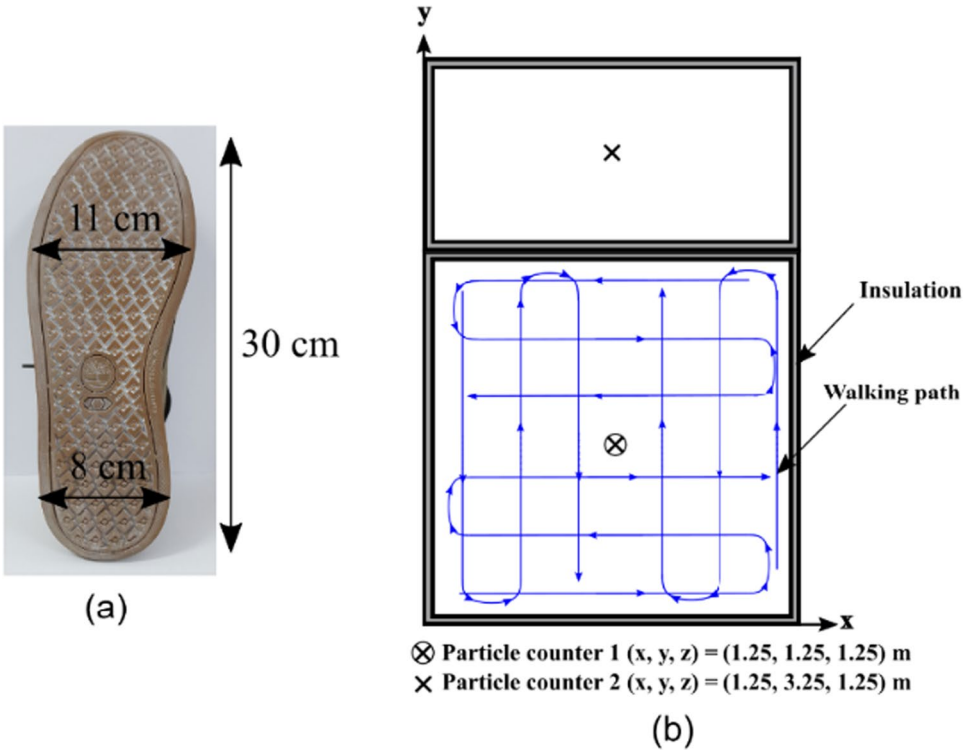

Fig. 5 **a** Dimensions of the shoe used during the experiments (42 EU and US), **b** top view of the experimental chambers showing particle monitors locations and the walking path

Table 3 Values of initial surface loading $L(0)$ for PM10, PM2.5, PM1, and PM0.1

PM	PM10	PM2.5	PM1	PM0.1
$L(0)$ (mg/cm^2)	6.50×10^2	6.08×10^2	5.12×10^2	2.73

additional times to evaluate the reproducibility of the procedure. In our approach, resuspension rates were calculated relative to the initial carpet loading (particle concentration on the carpet before the activity). We assumed that all particles aspirated during the loading assessment are susceptible to be resuspended. This assumption may lead to an overestimation of the charge term used in Eq. (1). Indeed, in a real environment and depending on the time the particle remains on the floor, the particle will sink further into the carpet and become unexposed to the airflow. This can reduce the possibility of its detachment by aerodynamic disturbances.

Results and analysis

The averaged mass of the collected powder of the three tests was equal to 0.7 ± 0.014 g/m^2. The initial alumina surface loading $L(0)$ values are represented in Table 3. This surface loading was deduced by assuming that floor loading particle size distributions did not change compared to that of the particles initially injected (see Fig. 3b).

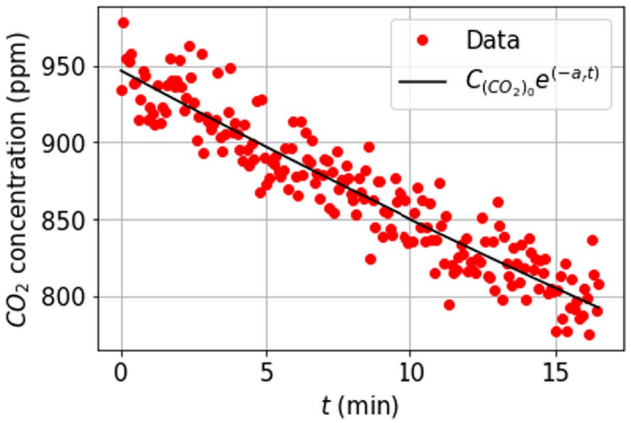

Fig. 6 CO_2 concentration evolution inside the test chamber. $C_{(CO_2)_0}$ represents the initial CO_2 concentration

Figure 6 shows the CO_2 concentration decay inside the chamber as a function of time and exponential curve fit. Accordingly, the renewal rate of the experimental chamber is constant and equal to 0.01 h^{-1}.

Figure 7a–d show concentration decays of PM inside the deposition chamber as a function of time and an exponential regression (the time $t=0$ min corresponds to the beginning of the particle decay) for a typical experiment. For each PM, the curve adjustment coefficient represents the loss rate coefficient.

Table 4 represents the loss rate coefficients of different PM ranges in the test chamber. As previously discussed,

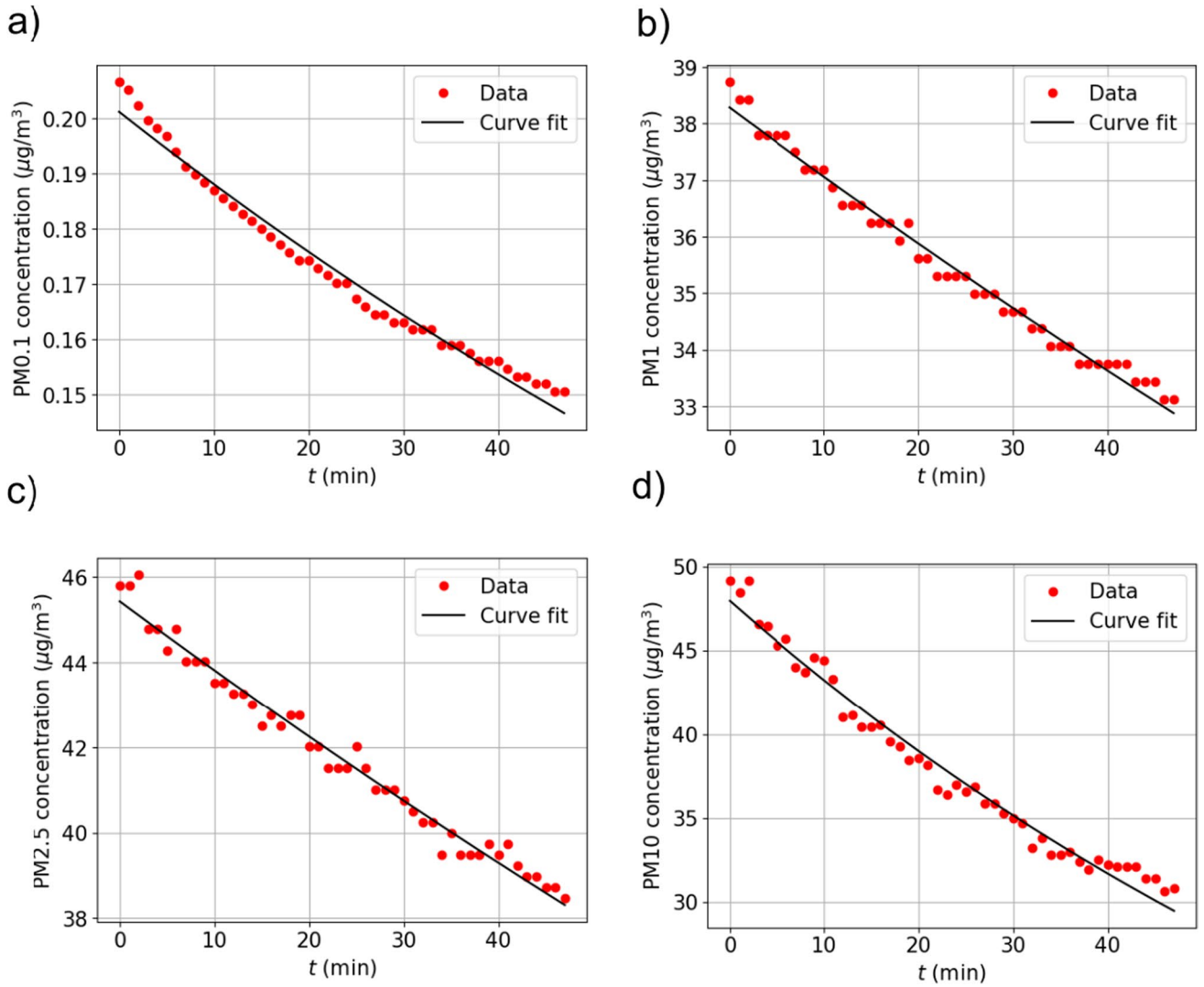

Fig. 7 PM deposition curves: **a** PM0.1, **b** PM1, **c** PM2.5, **d** PM10

Table 4 Loss rates for PM10, PM2.5, PM1, and PM0.1

PM	PM10	PM2.5	PM1	PM0.1
λ_{loss} (h^{-1})	1.5 ± 0.7	$(3.6 \pm 0.2) \times 10^{-1}$	$(2.4 \pm 0.3) \times 10^{-1}$	$(4.8 \pm 0.2) \times 10^{-1}$

the loss rate combines the effect of two phenomena on indoor particle concentration decrease: (1) particle deposition on the chamber internal surfaces and (2) the ventilation. Therefore, as the air change rate of the chamber is a constant, the difference in the loss rates between the different PM ranges is due to particle deposition. On the one hand, for PM10, PM2.5, and PM1 size ranges, particle deposition increases with particles size. On the other hand, for particle smaller than 0.1 µm, particle deposition is enhanced due to Brownian diffusion, turbulent diffusion, and electrostatic forces. Indeed, loss rate of PM10 is 4 and 6 times greater than those of PM2.5 and PM1 respectively and only 3 times greater than that of PM0.1.

The re-entrainment from clothing can be considered a particle source. This parameter was assumed to be negligible because the participant was wearing a clean coverall during the activity. This hypothesis has been tested experimentally. Figure 8 shows the change in PM10, PM2.5, PM1, and PM0.1 mass concentrations inside the test chamber during walking activity on zero load floor (cleaned floor). The participant started the activity at $t = 5$ min. We

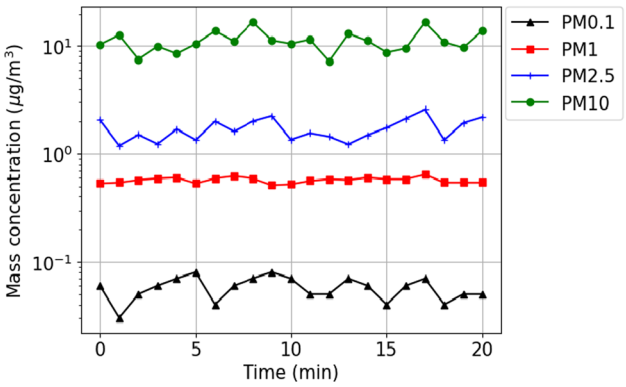

Fig. 8 Mass concentration versus time measured at a fixed location in the test chamber

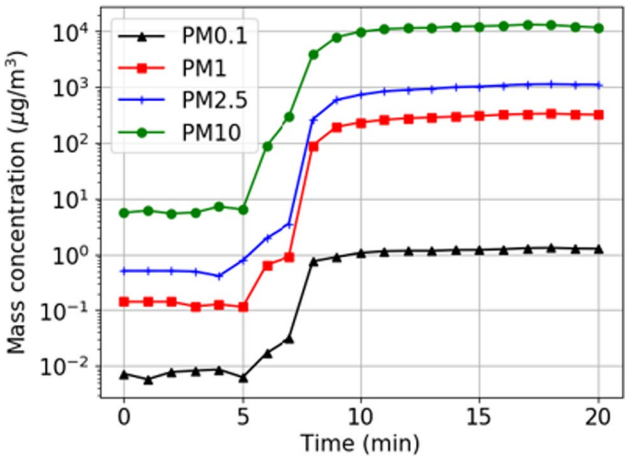

Fig. 9 PM10, PM2.5, PM1, and PM0.1 mass concentrations versus time measured at fixed locations in the test chamber

note that there is no variation in particle concentration which validates our hypothesis.

Figure 9 shows the time variation of PM10, PM2.5, PM1, and PM0.1 mass concentrations for a typical resuspension experiment. Accordingly, there was no variation on PM concentration between the times 0 min and 5 min which correspond to the instants at which the participant enters the test chamber and starts the activity, respectively. Profiles in Fig. 9 indicate also that the mass concentrations of all PM increase sharply by many orders of magnitude after the start of the activity (5–8 min) then increase slowly until the end of the activity at time 15 min. This result confirms that human walking contributes significantly to increase particle concentration in indoor environments. In addition, the present work has revealed that human activity can resuspend ultrafine particles represented by PM0.1. However, the evaluation of a resuspension coefficient is, therefore, necessary to evaluate the real resuspension emissions and to compare our results with those of the literature.

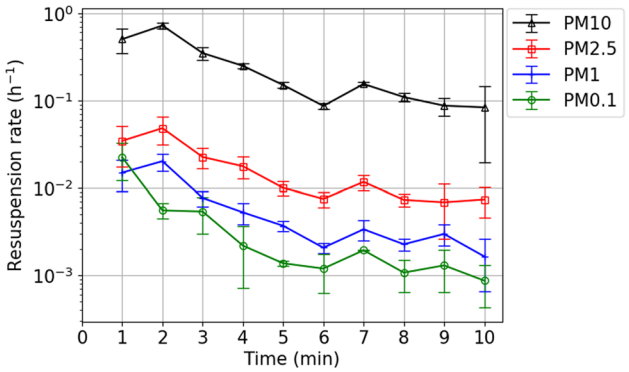

Fig. 10 PM10, PM2.5, PM1, and PM0.1 resuspension rates versus time. Error bars are standard deviations

Table 5 Values of resuspension rate for PM10, PM2.5, PM1, and PM0.1

$r_{rs,i}$ (h^{-1})	Present work 48 steps/min, RH = 40%	You and Wan (2015) 132 steps/min, RH = 82%
PM10	$(2.5 \pm 0.6) \times 10^{-1}$	5.1×10^{-1}
PM2.5	$(1.9 \pm 0.5) \times 10^{-2}$	2.0×10^{-1}
PM1	$(6.5 \pm 0.3) \times 10^{-3}$	/
PM0.1	$(4.3 \pm 0.3) \times 10^{-3}$	/

Resuspension during the participant walking period was quantified for each experiment. Figure 10 plots the estimated PM10, PM2.5, PM1, and PM0.1 resuspension during the walking period. The resuspension rates decrease with time for all PM. There is approximately one order of magnitude of difference between the resuspension rates of the first and the last moment. These decreases were due to a harvesting effect (Qian and Ferro 2008). Indeed, less tightly adhered particles are resuspended first, leaving more tightly adhered particles, which are not as easily resuspended. Figure 10 reveals also that at each instant, PM10 resuspension rate is greater by one order of magnitude than that of PM2.5 and approximately two orders of magnitude than those of PM1 and PM0.1.

In order to compare our results with those of the literature, we averaged the PM resuspension rates over time. It should be noted that literature provides no result on the resuspension rates of PM1 and PM0.1. Table 5 presents the estimated time-average resuspension rates and standard deviation for PM10, PM2.5, PM1, and PM0.1 from the present work, and PM10 and PM2.5 from the work of You and Wan (2015). Results of the present work show that the PM10 resuspension rate was one order of magnitude higher than that of PM2.5, and almost two orders of magnitude higher

than those of PM1 and PM0.1. These results confirm the observations made by previous works on the fact that particle resuspension increases as particle size decreases. This is probably due to the adhesion forces of the particles such as the electrostatic force which increases as particle size decreases (Feng and Hays 2003; Walton 2008).

Table 5 shows also that PM10 and PM2.5 resuspension rates of You and Wan (2015) are respectively two times and one order of magnitude greater than that of the present work. This is due on one hand to the walking rate of You and Wan (2015) which was about three times greater than that of the present work. On the other hand, this can be caused by the RH levels of the two studies. You and Wan (2015) suggest that the difference between resuspension rates under different RH is caused by the disappearance of meniscuses between the particles and flooring material due to humidity drop which leads to a greater reduction of the overall capillary forces.

Results of the present work show that human activity such as human walking could increase particle concentration of different sizes. However, the estimated resuspension rates cannot represent rates to be considered for any type of surface and any environmental conditions. Other parameters such as surface type, human walking intensity, and environmental conditions have a significant impact on resuspension and should be taken into account.

Conclusion

This study experimentally investigated the human walking–induced particle matter (PM) resuspension inside a full-scale chamber. The PM10, PM2.5, PM1, and PM0.1 resuspension rates during the walking activities were estimated by coupling two-compartment mass balance equations and by assuming a well-mixed condition inside the test chamber. Controlling all influencing parameters, such as floor loading, relative humidity, and outdoor particle concentration, allowed to reduce significantly the background concentration and to measure the evolution of particle concentration including the ultrafine particles.

This work revealed that human walking can contribute significantly to the increase in the concentration of particles including ultrafine particles (PM0.1). In addition, for the different size ranges, the resuspension rate increases with size. Indeed, the resuspension rate of PM10 is several orders of magnitude higher than that of PM2.5, PM1, and PM0.1. It was also found that PM resuspension rates decrease with time due to a harvesting effect (decrease in the concentration of particles on the ground after each participant pass).

As a perspective, it will be interesting to study the resuspension phenomenon in real environments and compare the contribution of human walking with other indoor sources. It is also important to study the influence of certain parameters such as surface type, walking speed, type of shoes, or environmental conditions on the phenomenon.

Author contribution All authors carried out the experiments and post-processed the experimental data.

All authors were involved in the manuscript preparation.

Funding The research project was financially supported by the Nouvelle Aquitaine region (CPER 2015–2020 Bâtiment Durable) and Health Agency (former ARS-Poitou–Charentes).

Data availability The manuscript has no associated data.

Declarations

Ethics approval and consent to participate Not applicable.

Consent for publication Not applicable.

Competing interests The authors declare no competing interests.

References

Araujo JA, Barajas B, Kleinman M et al (2008) Ambient particulate pollutants in the ultrafine range promote early atherosclerosis and systemic oxidative stress. Circ Res 102(5):589–596. https://doi.org/10.1161/CIRCRESAHA.107.164970

Benabed A, Boulbair A, Limam K (2020a) Experimental study of the human walking-induced fine and ultrafine particle resuspension in a test chamber. Build Environ 171:106655. https://doi.org/10.1016/j.buildenv.2020.106655

Benabed A, Limam K, Janssens B et al (2020b) Human foot tapping-induced particle resuspension in indoor environments: flooring hardness effect. Indoor Built Environ 29(2):230–239. https://doi.org/10.1177/1420326X19856054

Braniš M, Řezáčová P and Domasová M (2005) The effect of outdoor air and indoor human activity on mass concentrations of PM10, PM2.5, and PM1 in a classroom. Environ Res 99(2): 143–149. https://doi.org/10.1016/j.envres.2004.12.001.

Coccia M (2020) Factors determining the diffusion of COVID-19 and suggested strategy to prevent future accelerated viral infectivity similar to COVID. Sci Total Environ 729:138474. https://doi.org/10.1016/j.scitotenv.2020.138474

Conticini E, Frediani B, Caro D (2020) Can atmospheric pollution be considered a co-factor in extremely high level of SARS-CoV-2 lethality in Northern Italy? Environ Pollut 261:114465. https://doi.org/10.1016/j.envpol.2020.114465

Diaz-Sanchez D, Proietti L, Polosa R (2003) Diesel fumes and the rising prevalence of atopy: an urban legend? Curr Allergy Asthma Rep 3(2):146–152. https://doi.org/10.1007/s11882-003-0027-4

Feng JQ, Hays DA (2003) Relative importance of electrostatic forces on powder particles. Powder Technol 135–136:65–75. https://doi.org/10.1016/j.powtec.2003.08.005

Ferin J (1994) Pulmonary retention and clearance of particles. Toxicol Lett 72(1–3):121–125. https://doi.org/10.1016/0378-4274(94)90018-3

Lai ACK, Tian Y, Tsoi JYL et al (2017) Experimental study of the effect of shoes on particle resuspension from indoor flooring

materials. Build Environ 118:251–258. https://doi.org/10.1016/j.buildenv.2017.02.024

Luoma M, Batterman SA (2001) Characterization of particulate emissions from occupant activities in offices: characterization of particulate emissions from occupant activities in offices. Indoor Air 11(1):35–48. https://doi.org/10.1034/j.1600-0668.2001.011001035.x

Maher BA, Ahmed IAM, Karloukovski V et al (2016) Magnetite pollution nanoparticles in the human brain. Proc Natl Acad Sci 113(39):10797–10801. https://doi.org/10.1073/pnas.1605941113

Mendell MJ (2007) Indoor residential chemical emissions as risk factors for respiratory and allergic effects in children: a review. Indoor Air 17(4):259–277. https://doi.org/10.1111/j.1600-0668.2007.00478.x

Ogen Y (2020) Assessing nitrogen dioxide (NO2) levels as a contributing factor to coronavirus (COVID-19) fatality. Sci Total Environ 726:138605. https://doi.org/10.1016/j.scitotenv.2020.138605

Peters A, Wichmann HE, Tuch T et al (1997) Respiratory effects are associated with the number of ultrafine particles. Am J Respir Crit Care Med 155(4):1376–1383. https://doi.org/10.1164/ajrccm.155.4.9105082

Pope CA III (2002) Lung cancer, cardiopulmonary mortality, and long-term exposure to fine particulate air pollution. JAMA 287(9):1132. https://doi.org/10.1001/jama.287.9.1132

Qian J, Ferro AR (2008) Resuspension of dust particles in a chamber and associated environmental factors. Aerosol Sci Technol 42(7):566–578. https://doi.org/10.1080/02786820802220274

Serfozo N, Chatoutsidou SE, Lazaridis M (2014) The effect of particle resuspension during walking activity to PM 10 mass and number concentrations in an indoor microenvironment. Build Environ 82:180–189. https://doi.org/10.1016/j.buildenv.2014.08.017

Thatcher T (1995) Deposition, resuspension, and penetration of particles within a residence. Atmos Environ 29(13):1487–1497. https://doi.org/10.1016/1352-2310(95)00016-R

Verrier RL, Mittleman MA, Stone PH (2002) Air pollution: an insidious and pervasive component of cardiac risk. Circulation 106(8):890–892. https://doi.org/10.1161/01.CIR.0000027434.34445.23

Walton OR (2008) Review of adhesion fundamentals for micron-scale particles. KONA Powder Part J 26(0): 129–141. https://doi.org/10.14356/kona.2008012.

Wu X, Nethery RC, Sabath MB, et al (2020) Exposure to air pollution and COVID-19 mortality in the United States: A nationwide cross-sectional study. Preprint 7 April. Epidemiology. https://doi.org/10.1101/2020.04.05.20054502.

You S, Wan MP (2015) Experimental investigation and modelling of human-walking-induced particle resuspension. Indoor Built Environ 24(4):564–576. https://doi.org/10.1177/1420326X14526424